

UAV Assisted USV Visual Navigation for Marine Mass Casualty Incident Response

Xuesu Xiao^{1,*}, Jan Dufek^{1,*}, Tim Woodbury^{2,*}, and Robin Murphy¹

Abstract—This research teams an Unmanned Surface Vehicle (USV) with an Unmanned Aerial Vehicle (UAV) to augment and automate marine mass casualty incident search and rescue in emergency response phase. The demand for real-time responsiveness of those missions requires fast and comprehensive situational awareness and precise operations, which are challenging to achieve because of the large area and the flat nature of the water field. The responders, drowning victims, and rescue vehicle are far apart and all located at the sea level. The long distances mean responders cannot clearly discern the rescue vehicle and victims from the surrounding water. Furthermore, being at the same elevation makes depth perception difficult. Rescue vehicle and victims at different distances from the responder will always appear to be close together. This makes it almost impossible for the responders to accurately drive the USV to the victims in time. This paper proposes the use of a UAV to compensate for the lack of elevation of the responders and to automate search and rescue operations. The benefit of this system is two fold: 1) the UAV provides responders with an overhead view of the field, covers larger area than direct visual, and allows more accurate perception of the situation, and 2) it automates the rescue process so that the responders can focus on task-level needs instead of tediously driving the USV to the victims. Thirty autonomous navigation trials in 4 rescue scenarios prove the first known successful implementation of a small UAV visually navigating a USV.

I. INTRODUCTION

Unmanned Surface Vehicles (USVs) have been used since 2004 for disaster recovery operations [1]. Multiple USVs, including Unmanned Marine Vehicles (UMVs), underwater Remotely Operated Vehicles (ROVs), and Autonomous Underwater Vehicles (AUVs), were deployed in Hurricane Wilma [2] [3], Hurricane Ike [4], Tohoku Earthquake and Tsunami [1] [5]. The applications of deploying USVs for emergency response mainly focus on the recovery phase of disaster management, such as port and littoral damage inspection [4], safe lanes for sea navigation [2], hazardous materials spills detection, or serving as a wireless network relay [3]. Other applications include a new type of Simultaneous Localization and Mapping (SLAM) with vision both above and below the waterline [3], port clearing, and victim recovery [1] [5]. However, this focus on using USVs for structural and economic recovery neglects the usability of those vehicles in the response phase, especially for victim

¹Xuesu Xiao, Jan Dufek, and Robin Murphy are with the Department of Computer Science and Engineering, Texas A&M University, College Station, Texas 77843 xiaoxuesu@tamu.edu, dufek@tamu.edu, murphy@cse.tamu.edu

²Tim Woodbury is with the Department of Aerospace Engineering, Texas A&M University, College Station, Texas 77843 twoodbury@tamu.edu

*Equally contributing authors



Fig. 1. Actual problem encountered by marine mass casualty rescuers: view point from USV operator. The USV and victim are not discernible from the view point at limited altitude on shore. Objects may actually be far apart, especially in perpendicular direction to shore, even though they appear to be very close due to perspective effect.

search and rescue, where the real-time responsiveness is much more critical. For example, the coastline search and rescue mission taking place in Lesbos, Greece, is to save refugees from drowning. Response time is critical for victims in danger, and USVs could reach the victim faster than a human rescuer. USVs can provide flotation to conscious victims, deliver rescue lines to boats in trouble, and give guidance for boats to a safer location. USVs can also be used to attend to less urgent victims, while human lifeguards swim to aid the people who need special professional attention. The state-of-art practice of using USV for marine mass casualty search and rescue is mainly based on manual operation. The rescuers use a remote controller to drive the USV to victims. However, this approach is subject to challenges caused by human's limited perception capability: human eyes cannot see very far from shore and the limited height makes depth perception difficult. Fig. 1 is the view from a USV operator. It is almost impossible to clearly discern where the USV and victims are. Depth perception is even more challenging because USV and victims can appear to be very close to each other even if they are at completely different distances from operator. This work mainly aims at solving this problem in marine mass casualty response and use autonomy to largely improve the responders' efficiency. To the authors' knowledge, this is the first known implementation of a small UAV visually navigating a USV.

II. RELATED WORK

Using both Unmanned Aerial and Ground Vehicle in heterogeneous robot teams is not a brand new topic. In

[6], a certain area is searched by a UAV-UGV team. Teams of UGVs are responsible for monitoring map cell border, while UAVs scan each individual cell. In [7], researchers look into a hierarchical way for UAV-UGV cooperation. Based on the better situation awareness provided by the UAV's high altitude, a top-level mobile mission controller is implemented to guarantee better system-level decision making. More researchers pay attention to closer cooperation between UAV and UGV, mostly in a lower-level sensing or sense/act scenario. UAVs are usually used to assist the UGV. In [8], a blimp provides overhead view over a stadium, where the UGV's location could be more effectively estimated by visual cues. UAV and UGV teams are also used for radio map construction [9] and image plane calibration [10]. Those work shows that a UAV with vision capability can improve the system's situation awareness. This paper applies this idea from ground to marine surface to solve a new marine mass casualty search and rescue problem, and extends the rescuer's capability into areas which in current practice are not possible with only human operators. Furthermore, our method can also directly initiate the locomotion of the USV and thus frees the operator from tedious manual control. The responders could then focus on more critical task-level needs.

The control of an unmanned vehicle by a UAV has also been explored in the literature. In particular, Rao, Kumar, and Taylor offer promising results that the control of a ground vehicle from an aerial overview is differentially flat given the camera system is well calibrated [11]. However, the result of this work is only demonstrated in simulation. Based on [11], physical experiments are conducted, but only in controlled indoor lab environment, where the homography that relates the image plane to the ground plane is easy to calibrate [12]. [13] conducted outdoor physical experiments, but the UAV's partner is only a UGV moving on stable and thus less challenging solid flat ground. In this paper, a USV is controlled by a UAV in physical experiments conducted in outdoor open water area (Fig. 2). The uncontrollable environmental factors, such as variations in wind, wave, and illumination conditions, makes camera calibration difficult and cause challenges in control, tracking, and robustness. Furthermore, the nature of search and rescue missions in emergency response requires real-time and fast responsiveness of our system. To the authors' knowledge, this is the first known implementation of a UAV visually navigating a USV.

The paper is organized as follows: Section II discusses the previous work. In Section III, the heterogeneous robot team is introduced. Section IV and Section V describe the USV's tracker and controller respectively. The experimental results are presented in Section VI. Section VII concludes the paper.

III. SYSTEM OVERVIEW

Our system is composed of a USV, designated EMILY (Emergency Integrated Lifesaving Lanyard), a UAV (Fotokite), ground stations for both vehicles, and a tracking-control system (network) that bridges the two platforms. However, in general, any UAV platforms with online visual feed and USVs with rudder and throttle control could be used



Fig. 2. EMILY visual navigation in Galveston Bay, Texas under strong wind (17km/h) and current

in our approach. Our system is in a "plug-and-play" setting, independent of the particular robots used by the responders. Therefore, the contribution of this paper is a working system configuration compatible with a variety of commercially available robotic platforms. This system is fieldable and can solve a real-life search and rescue problem and improve response efficiency, which are, to our knowledge, impossible in current practice with only human rescuers.

A. EMILY

In conventional water rescue missions, rescue boats 1) are operated by a human captain onboard and 2) carry victims to land. In this work, a USV, EMILY (Fig. 1), is remotely controlled by the operator, or automatically navigates either using GPS or overhead visual. Furthermore, instead of carrying the victims back, EMILY can approach the victims and then serve as a buoy. EMILY can either provide flotation until a rescuer arrives, deliver life jackets, or pull a recovery rescue line up to 800 feet through strong currents and large surf. The main advantage of deploying EMILY is the fast response time. This 1.2m long remote controlled buoy can cruise through rip-currents and swift water at speeds up to 35 km/h to reach distressed swimmers faster than a swimming human lifeguard. For propulsion, EMILY uses a steerable jet pump with inlet grate. This mechanism has the dual advantages of being safer for the victims than an external propellor, and will not bind up on rocks or sand [14]. Four possible scenarios where EMILY can help are as follows: 1) getting flotation to victims and then pulling them to the rescue boat or shore, 2) bringing a rescue line to a boat in trouble, 3) providing a target for a manned boat to follow to a safer area, 4) allowing human lifeguards to swim to aid the victims who need special professional attention, while EMILY goes to the people who are still able to grab on. All four applications require a precise and comprehensive situational awareness, which cannot be guaranteed by human visual observation from distance.

We augment EMILY's standard remote controller with a Pixhawk autopilot. This provide us with an interface to more autonomous capabilities. The autopilot communicates to its

ground station via 915 MHz radio. On the base station, We use Mission Planner. It provides a graphical user interface to the remote vehicle. Remote control, GPS waypoints navigation, and any custom developed autonomous functionalities are integrated in the Pixhawk and Mission Planner setup, including our UAV visually assisted navigation. Return To Home (RTH) functionality is a failsafe for situations where EMILY is out of the radio range, radio interference is strong on site, or the radio communications link is otherwise disrupted.

B. Fotokite

The ability of small four-rotor VTOL (Vertical Take-Off and Landing) UAV to hover is desirable for a wide range of applications like searching, surveillance and reconnaissance missions. The visual feedback provided by the on-board camera can give an overhead view above the field, and thus give valuable information about the scenario. In this work, a four-rotor tethered UAV, Fotokite Pro, is used to serve as a visual assistant to the USV, EMILY. The tether is used for power transmission from the ground station and safety. This can largely reduce the weight for the battery onboard, thus extending the flight time and making the aircraft more agile. Other than Fotokite used in this work, any rotorcraft with live video feed could play the role of visual assistant for this particular application (such as DJI Inspire in Fig. 2).

On the Fotokite ground station, operator can control the drone using different control joysticks and command the aircraft to hover at a certain position. The video is streamed from the GoPro camera onboard to the ground station. The ground station provides an HDMI port for video output, which we can use for tracking and control purposes [15].

C. System Setup

In this heterogeneous robot team, the USV and UAV are connected by a network, which extends from the rescuers, to the water surface and air, as shown in Fig. 3.

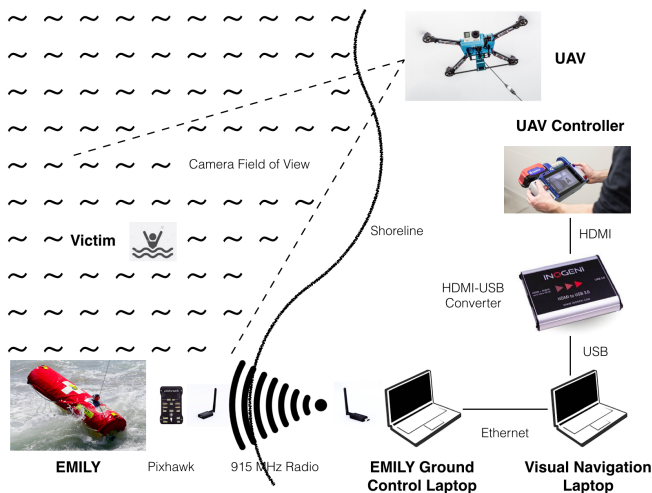


Fig. 3. System Setup

Fotokite is automatically hovering in the air above the area of interest. EMILY and as many victims as possible

should fit in the field of view of the UAV's onboard camera. Both position and altitude of the drone are important. The location should cover as many objects of interest as possible, and the altitude determines the coverage of the scene and the difficulty in tracking, since the higher the drone is, the fewer pixels the objects occupy in the image, and thus more difficult it is for the tracking algorithm.

The GoPro video is streamed from the drone to the ground station. The video is sent via the HDMI output to Inogeni HDMI-USB Converter that makes the video ready for any laptop with USB ports. A laptop takes in the video stream and runs the tracking algorithm. The tracking outputs the position and orientation of EMILY in the image frame, which are passed to the controller. The controller then calculates the rudder and throttle commands based on EMILY's current position and orientation, and the victim's location, which could be more precisely defined by the operator due to his/her enhanced situation awareness provided by the UAV.

The rudder and throttle commands are then sent via Ethernet to another laptop running Mission Planner. Mission planner is able to transmit those commands via 915 Mhz radio to EMILY. The Pixhawk onboard takes the commands from its antenna and controls the steering servo and jet motor to approach the victim.

IV. VISUAL TRACKING

Visual tracking extends on [16], where error of only a few pixels in a full HD video feed already proved the sufficient accuracy for EMILY position tracking. We improve the orientation tracking by Douglas-Peucker algorithm [17]. A "warping" function for oblique camera view is added to face the situation where the UAV is not high enough so only an oblique view is available. It is not to say other more sophisticated tracking methods such as Deep Neural Networks or feature based template tracking are not helpful in our system, but the histogram-based blob tracking works robustly enough in all our field experiments. This suffices for the preliminary result of a fieldable working system.

A. Position Estimation

Unlike indoor or controlled environments, video feed in each rescue mission varies with different locations, illumination, weather conditions, etc, so we use human intelligence to initialize tracking with a selected template. After hue histogram backprojection detection, CamShift algorithm [18] is applied to guarantee smooth tracking. The centroid of the CamShift window is taken as the centroid of EMILY.

B. Orientation Estimation

Estimation based on blob shape analysis [16] is proved to be not precise enough to enable reliable navigation in our field experiments. Orientation is estimated by using the movement history. The position of EMILY in the image is recorded over time. To handle the jerky motion caused by noise, we use Douglas-Peucker algorithm to approximate the movement with a curve with fewer vertices. This filters out the noise and leaves a smoother trajectory. A tangent at the

last point of the approximated curve is computed as the orientation.

C. Homogeneous Transformation

Sometimes the UAV is not hovering at a high altitude or it has to stay above the shoreline due to FAA regulations, then instead of a perfect overhead shot an oblique view is the best input to the visual tracker. While tracking of horizontal motions in the oblique image frame is still precise enough, vertical motion, especially when EMILY is far away from camera, is not easy to discern by the tracker due to perspective effect. To resolve this, we add homogeneous transformation, which is based on an estimation of the oblique angle. The “inverse perspective warping” can “enlarge” the diminished distant areas so that EMILY’s motion could be easily recognized. Experiment results suggest that “warping” function enables vertical navigation, which is impossible to achieve in some very oblique view points without “warping”.

D. Graphical User Interface

The graphical user interface (Fig. 4) was designed to make it easier to set parameters (using sliders) and see the navigation progress. Tracking, warping, and control parameters can be set instantly based on different rescue scenarios. Both EMILY and target can be selected on the fly to increase responsiveness. The operator can monitor the progress of tracking (including visualization of position, orientation, shape, and trajectory of EMILY) and see the histogram and backprojection.

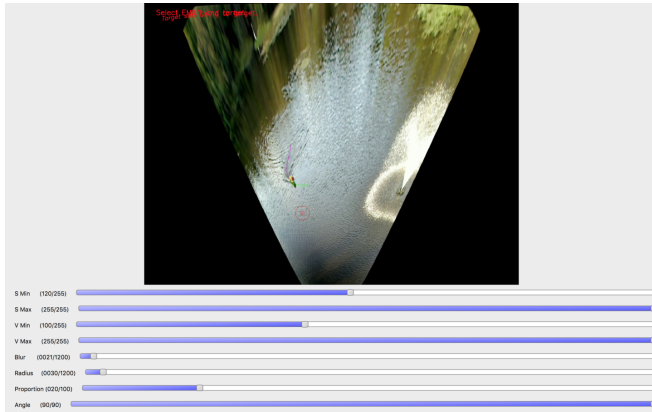


Fig. 4. Tracking User Interface

V. CONTROL

To navigate EMILY to desired victim location, the system uses line-of-sight for high-level control and PID for USV heading direction.

A. Line-of-sight Control

Line-of-sight control is used in this work considering the system’s online and physical implementation requirement. Line-of-sight control is a well-developed control strategy for path following. Previous work looked into the stability [19], implementation [20], and control laws for this technique [21].

It is not only suitable for conventional mobile systems [22] or under-actuated vehicles [23], it has also been used to navigate hyper redundant locomotors, such as snake robots [24], along a predefined path. Therefore the line-of-sight control strategy suffices for this particular application as well.

The planned path for the USV is an ordered set of target points, which are denoted by P_n . At each time step, P_{k-1} denotes the previous target point visited by the USV while P_k designates the current target point, as shown in Fig. 5. The two consecutive waypoints P_{k-1} and P_k are connected by a straight line segment. A circle with radius L around the USV intersects with that line segment at two points. Between these two points, we designate the one closer to the next target point, P_k , as line-of-sight point, P_{los} . The line-of-sight point is the point which the controller aims toward at every single time step. A circle with radius R_k is defined as the circle of acceptance around P_k . When the USV is within this circle, it means the robot already arrived at this particular waypoint and the next target waypoint is updated to P_{k+1} .

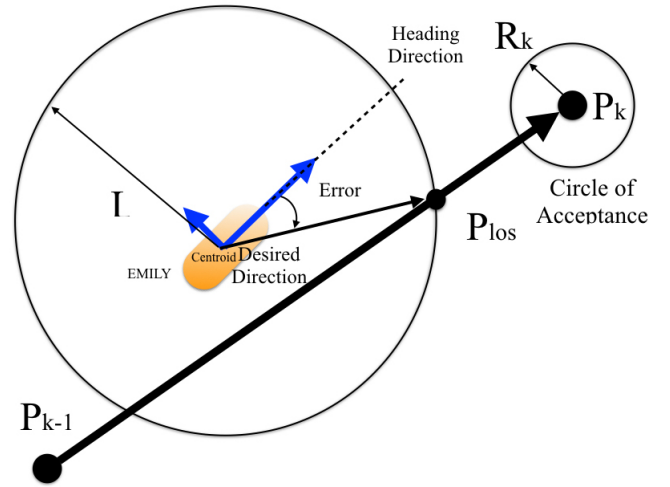


Fig. 5. Line-of-sight control based on heading error angle

B. Rudder and Throttle Control

After the high level line-of-sight navigation is defined, the control strategy is specified to move the USV toward the line of sight point, and thus lead it to the victim. There are two control regimes, which are discussed subsequently.

1) *Turning Mode*: When the error angle (Fig. 5) is greater than 30° , the controller is in turning mode. The rudder is set to the maximum value aiming toward the target point and only 30% of the maximum throttle is applied. This imitates the “turn in place” motion of differential-drive vehicles. But the non-holonomic USV has a small turning radius.

2) *PID Mode*: When the error angle (Fig. 5) is within the 30° threshold, proportional-integral-derivative (PID) control is used to achieve a desired heading. Throttle is set to 60% of the maximum value.

C. Throttle Control

In addition to the two modes mentioned above, to ensure safety, EMILY decelerates when approaching the victims by

setting the throttle value proportional to the distance to target.

VI. EXPERIMENTS

To test the performance of the proposed system, experiments are conducted on both GPS and visual navigation in Galveston Bay, Galveston, TX (Fig. 2), Lake Bryan, Bryan, TX (Fig. 6(a)), John Crompton Park, College Station, TX (Fig. 6(b)), and Porto Antico di Genova, Genoa, Italy. GPS navigation is not applicable for our search and rescue scenario since the GPS coordinates of the victim is not available for our navigator. However the GPS data are used as ground truth to evaluate the visual navigation results since we can extract GPS coordinates when EMILY reaches target.

In Fig. 2, one EMILY's visual navigation trial is shown. EMILY's position and orientation at different time frames are overlaid to one single overhead view from the UAV. The high altitude of the UAV provides an almost vertical view of the scene. However, the constantly changing strong wind and wave in the bay area causes challenges for the controller resulting in a curved trajectory. Results for two example visual trials in Lake Bryan and John Crompton Park are presented in Fig. 6(a) and Fig. 6(b) without and with "warping". The ground truth in GPS frame is presented for the latter. The relations between the USV's actual movement and the parameter profiles are illustrated.

In Fig. 6(a), EMILY turns around after initialization, because the heading direction is opposite to the target at the beginning. After that, the system is in PID mode. Before reaching the target, the error angle exceeds the threshold, so the controller is in turning mode again to orient the heading of EMILY within the 30° range of the target. EMILY reaches the target in PID mode and decelerate. Distances are in image coordinates.

With a lower camera altitude and larger oblique angle (Fig. 6(b)), "warping" is used to rectify the image to an approximated overhead view. It can navigate along the vertical image direction, which is impossible without "warping". Distances are in GPS frame.

In both cases, the PID-controller controls the rudder and throttle to reduce the absolute value of Emily's error angle. It oscillates around zero along the entire path. The distance to target is continuously reduced while EMILY is approaching the target. The distance to the ideal straight line path also oscillates due to the nature of the PID-controller and environmental disturbances (wind and wave). We analyze this cross track error in detail. The throttle and rudder profiles also match with the control strategy and USV movement.

Results of experiments conducted in Galveston Bay, Lake Bryan, John Crompton Park, and Porto Antico di Genova, are summarized in Tab. I. Each test contains multiple visual navigation runs and in all runs EMILY successfully navigates to the target. We compute the cross track error as the distance between EMILY's ground truth GPS position to the ideal straight line path. The maximum cross track error is very sensitive to the initial heading. Because EMILY is non-holonomic, turning around largely increases the maximum cross track error if its initial heading is in opposite direction

from the target. The wind condition also has a strong effect on the average and maximum cross track error, especially in open water area with strong wind and current.

VII. CONCLUSIONS

In this paper a novel USV-UAV heterogeneous robotic team for automatic marine mass casualty response is proposed, designed, and implemented. The overhead view compensates for the lack of elevation of human responders on shore, thus makes search and rescue in distant water areas possible, and also increases situation awareness and operation precision of the rescue vehicle. The tracking system is adjustable to different environments so as to make the system applicable to a wide range of real-world scenarios. The controller allows the USV to navigate to the target victim location automatically and therefore frees operators from tedious remote control of the robot, allowing them to concentrate on more urgent or task-level needs. The system is actually fielded in 4 rescue scenarios.

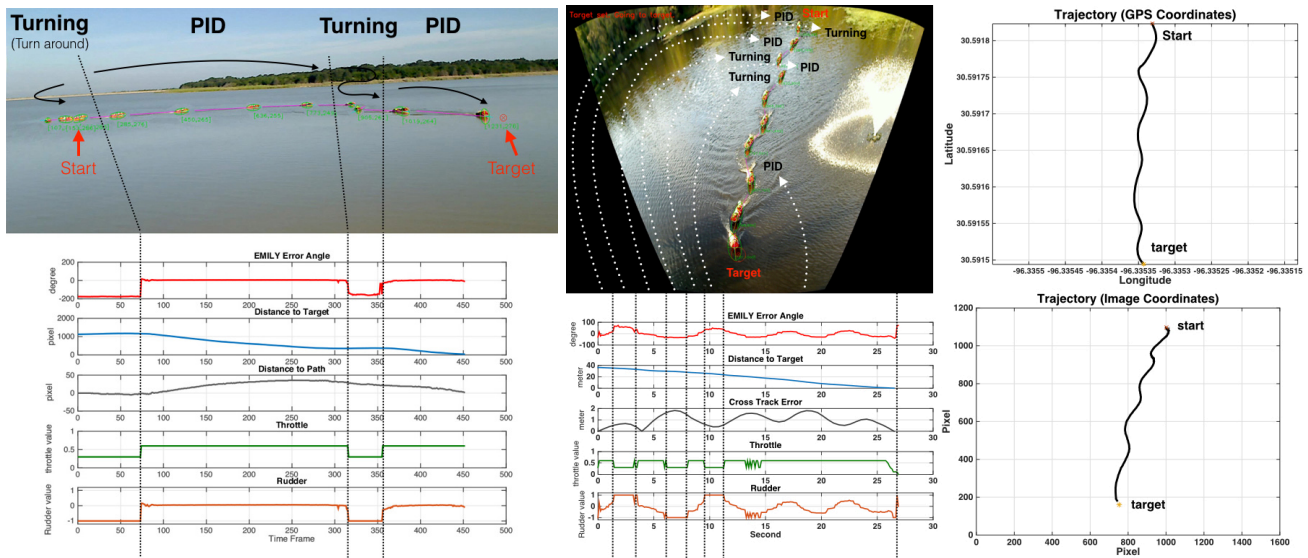
Although being proved to be fieldable and useful in real marine mass casualty search and rescue missions, this paper is only the preliminary result of this novel approach. Our system can expand the search and rescue coverage to distant regions previously inaccessible with pure human power. But in close water areas where both automation and manual control are possible, we need to demonstrate our system is a reliable substitute for human. Clearly human operators cannot easily drive EMILY in a perfect straight line to the victims either, but their performance needs to be quantified and compared with our system. The movement of the UAV in strong wind should be incorporated into the controller and possibly taken advantage of in future research.

ACKNOWLEDGEMENT

This work is supported by NSF OISE-1637214, RAPID: Using an Unmanned Aerial Vehicle and Increased Autonomy to Improve an Unmanned Marine Vehicle Lifeguard Assistant Robot.

REFERENCES

- [1] R. R. Murphy, K. L. Dreger, S. Newsome, J. Rodocker, E. Steimle, T. Kimura, K. Makabe, F. Matsuno, S. Tadokoro, and K. Kon, "Use of remotely operated marine vehicles at minamisanriku and rikuzentakata japan for disaster recovery," in *2011 IEEE International Symposium on Safety, Security, and Rescue Robotics*. IEEE, 2011, pp. 19–25.
- [2] R. R. Murphy, E. Steimle, C. Griffin, C. Cullins, M. Hall, and K. Pratt, "Cooperative use of unmanned sea surface and micro aerial vehicles at hurricane wilma," *Journal of Field Robotics*, vol. 25, no. 3, pp. 164–180, 2008.
- [3] R. Murphy, S. Stover, K. Pratt, and C. Griffin, "Cooperative damage inspection with unmanned surface vehicle and micro unmanned aerial vehicle at hurricane wilma," in *2006 IEEE/RSJ International Conference on Intelligent Robots and Systems*. IEEE, 2006, pp. 9–9.
- [4] E. T. Steimle, R. R. Murphy, M. Lindemuth, and M. L. Hall, "Unmanned marine vehicle use at hurricanes wilma and ike," in *OCEANS 2009*. IEEE, 2009, pp. 1–6.
- [5] R. R. Murphy, K. L. Dreger, S. Newsome, J. Rodocker, B. Slaughter, R. Smith, E. Steimle, T. Kimura, K. Makabe, K. Kon *et al.*, "Marine heterogeneous multirobot systems at the great eastern japan tsunami recovery," *Journal of Field Robotics*, vol. 29, no. 5, pp. 819–831, 2012.
- [6] H. G. Tanner, "Switched uav-ugv cooperation scheme for target detection," in *Proceedings 2007 IEEE International Conference on Robotics and Automation*. IEEE, 2007, pp. 3457–3462.



(a) Visual Trials at Lake Bryan, Bryan, TX, with data processed in camera image frame (b) Visual Trials at John Crompton Park, College Station, TX, with data processed in GPS coordinates

Fig. 6. Two Example Visual Trials

TABLE I
VISUAL NAVIGATION RESULTS

	Test 1	Test 2	Test 3	Test 4
Location	Galveston	Bryan	College Station	Genoa
Water Body	Sea	Lake	Pond	Sea
Wind Speed	17km/h South	11km/h East	0km/h	13km/h Northeast
Mean Cross Track Error	5.5m	4.6m	1.0m	1.9m
Maximum Cross Track Error	15.7m	20.5m	4.8m	4.9m
Number of Runs	1	14	11	4
Total Distance	23.8m	425.0m	293.7m	85.9m
Total Time	178s	562s	379s	121s

[7] C. Phan and H. H. Liu, "A cooperative uav/ugv platform for wildfire detection and fighting," in *System Simulation and Scientific Computing, 2008. ICSC 2008. Asia Simulation Conference-7th International Conference on*. IEEE, 2008, pp. 494–498.

[8] L. Chaimowicz, B. Grocholsky, J. F. Keller, V. Kumar, and C. J. Taylor, "Experiments in multirobot air-ground coordination," in *Robotics and Automation, 2004. Proceedings. ICRA'04. 2004 IEEE International Conference on*, vol. 4. IEEE, 2004, pp. 4053–4058.

[9] L. Chaimowicz, A. Cowley, D. Gomez-Ibanez, B. Grocholsky, M. Hsieh, H. Hsu, J. Keller, V. Kumar, R. Swaminathan, and C. Taylor, "Deploying air-ground multi-robot teams in urban environments," in *Multi-Robot Systems. From Swarms to Intelligent Automata Volume III*. Springer, 2005, pp. 223–234.

[10] R. Rao, C. J. Taylor, and V. Kumar, "Calibrating an air-ground control system from motion correspondences," in *Computer Vision and Pattern Recognition, 2004. CVPR 2004. Proceedings of the 2004 IEEE Computer Society Conference on*, vol. 2. IEEE, 2004, pp. II–218.

[11] R. Rao, V. Kumar, and C. Taylor, "Visual servoing of a ugv from a uav using differential flatness," in *Intelligent Robots and Systems, 2003.(IROS 2003). Proceedings. 2003 IEEE/RSJ International Conference on*, vol. 1. IEEE, 2003, pp. 743–748.

[12] R. S. Rao, V. Kumar, and C. J. Taylor, "Planning and control of mobile robots in image space from overhead cameras," in *Proceedings of the 2005 IEEE International Conference on Robotics and Automation*. IEEE, 2005, pp. 2185–2190.

[13] N. Frietsch, O. Meister, C. Schlaile, and G. Trommer, "Teaming of an ugv with a vtol-uav in urban environments," in *2008 IEEE/ION Position, Location and Navigation Symposium*. IEEE, 2008, pp. 1278–1285.

[14] Hydronalix. Emergency integrated lifesaving lanyard. [Online]. Available: <http://emilyrobot.com/>

[15] Perspective_Robotics_AG. Fotokite. [Online]. Available: <http://fotokite.com/>

[16] J. Dufek and R. R. Murphy, "Visual pose estimation of USV from UAV to assist drowning victims recovery," in *2016 IEEE International Symposium on Safety, Security and Rescue Robotics*. IEEE, 2016.

[17] D. H. Douglas and T. K. Peucker, "Algorithms for the reduction of the number of points required to represent a digitized line or its caricature," *Cartographica: The International Journal for Geographic Information and Geovisualization*, vol. 10, no. 2, pp. 112–122, 1973.

[18] G. R. Bradski, "Computer vision face tracking for use in a perceptual user interface," 1998.

[19] P. J. Kennedy and R. L. Kennedy, "Direct versus indirect line of sight (los) stabilization," *IEEE Transactions on control systems technology*, vol. 11, no. 1, pp. 3–15, 2003.

[20] J. Waldmann, "Line-of-sight rate estimation and linearizing control of an imaging seeker in a tactical missile guided by proportional navigation," *IEEE Transactions on control systems technology*, vol. 10, no. 4, pp. 556–567, 2002.

[21] K. Lim and G. Balas, "Line-of-sight control of the csi evolutionary model: μ control," in *American Control Conference, 1992*. IEEE, 1992, pp. 1996–2000.

[22] H. Yoon and P. Tsiotras, "Spacecraft line-of-sight control using a single variable-speed control moment gyro," *Journal of guidance, control, and dynamics*, vol. 29, no. 6, pp. 1295–1308, 2006.

[23] T. I. Fossen, M. Breivik, and R. Skjetne, "Line-of-sight path following of underactuated marine craft," *Proceedings of the 6th IFAC MCMC, Girona, Spain*, pp. 244–249, 2003.

[24] X. Xiao, E. Cappo, W. Zhen, J. Dai, K. Sun, C. Gong, M. J. Travers, and H. Choset, "Locomotive reduction for snake robots," in *2015 IEEE International Conference on Robotics and Automation (ICRA)*. IEEE, 2015, pp. 3735–3740.